Talanta 208 (2020) 120452

Contents lists available at ScienceDirect

Talanta

journal homepage: www.elsevier.com/locate/talanta

Quantum dots are conventionally applicable for wide-profiling of wall polymer distribution and destruction in diverse cells of rice

Qiaomei Yang[a,b,f], Wenyue Zhao[a,b,f], Jingyuan Liu[a,b], Boyang He[a,b], Youmei Wang[a,c], Tangbin Yang[d], Guifen Zhang[a,b], Mingxiong He[e], Jun Lu[f], Liangcai Peng[a,b,f], Yanting Wang[a,b,f,*]

[a] Biomass and Bioenergy Research Centre, Huazhong Agricultural University, Wuhan, China
[b] College of Plant Science and Technology, Huazhong Agricultural University, Wuhan, China
[c] College of Life Science and Technology, Huazhong Agricultural University, Wuhan, China
[d] Beijing Najing Biotechnology Co., Ltd, Wuhan, China
[e] Key Laboratory of Development and Application of Rural Renewable Energy, Ministry of Agriculture and Rural Affairs, Chengdu, China
[f] Laboratory of Biomass Engineering and Nanomaterial Application in Automobiles, College of Food Science and Chemical Engineering, Hubei University of Arts and Science, Xiangyang, China

ARTICLE INFO

Keywords:
Glycan immunolabeling
Quantum dots
Chemical pretreatment
Plant cell wall
Biomass
Rice

ABSTRACT

Plant cell walls represent enormous biomass resources for biofuels, and it thus becomes important to establish a sensitive and wide-applicable approach to visualize wall polymer distribution and destruction during plant growth and biomass process. Despite quantum dots (QDs) have been applied to label biological specimens, little is reported about its application in plant cell walls. Here, semiconductor QDs (CdSe/ZnS) were employed to label the secondary antibody directed to the epitopes of pectin or xylan, and sorted out the optimal conditions for visualizing two polysaccharides distribution in cell walls of rice stem. Meanwhile, the established QDs approach could simultaneously highlight wall polysaccharides and lignin co-localization in different cell types. Notably, this work demonstrated that the QDs labeling was sensitive to profile distinctive wall polymer destruction between alkali and acid pretreatments with stem tissues of rice. Hence, this study has provided a powerful tool to characterize wall polymer functions in plant growth and development *in vivo*, as well as their distinct roles during biomass process *in vitro*.

1. Introduction

Plant cell walls are mainly composed of cellulose, hemicellulose, lignin and pectin, providing enormous biomass resources for biofuels and chemical production [1,2]. Due to lignocellulose recalcitrance, however, current biomass process is unacceptably costly for biofuels production [3]. To reduce recalcitrance, genetic modification of plant cell walls has been considered in bioenergy crops [[4–6]]. Meanwhile, acid and alkali pretreatments have been broadly applied to destruct wall polymers for sequentially enhanced biomass enzymatic saccharification [7,8]. Hence, it becomes important to find out an applicable technique for specific observation of wall polymers *in situ* during plant growth *in vivo* and biomass process *in vitro*. However, because plant cell walls are of complicated structures and diverse functions, it remains a technique difficulty to observe individual wall polymer distribution in specific tissue or to explore wall polymer destruction in single plant cells during biomass pretreatment and enzymatic saccharification.

Fluorescent probes are powerful tools to monitor dynamics and deconstruction of molecular architecture [[9–11]]. Glycan-directed antibodies have been applied to *in situ* observe wall polysaccharide profiling at the cellular level in order to gain their biological functions [[12–16]]. However, this technology could only detect individual wall polysaccharide in one dissection of plant tissues. Quantum dots (QDs), also known as semiconductor nanocrystals, are new type of fluorophores. The QDs commonly used in biological and medical applications are comprised of an inner core (CdSe), a shell (ZnS), and a surface coating which is used to increase stability and solubility [[17–21]]. Compare to organic fluorophores, QDs have high brightness, large stoke shift, and improved photo-stability [[21–23]]. More importantly, multi-fluorescent imaging can be obtained by labeling varieties of target sites simultaneously [24,25].

Since QDs were first used as fluorescent probes [26,27], this

* Corresponding author. Biomass and Bioenergy Research Centre, Huazhong Agricultural University, Wuhan 430070, China.
E-mail address: wyt@mail.hzau.edu.cn (Y. Wang).
URL: http://bbrc.hzau.edu.cn (Y. Wang).

https://doi.org/10.1016/j.talanta.2019.120452
Received 13 August 2019; Received in revised form 30 September 2019; Accepted 6 October 2019
Available online 07 October 2019
0039-9140/

approach has been widely applied in mammalian and human studies [[28–30]]. However, very little is reported about their applications in plant cell walls, probably due to their resistance to QD penetration [[24,31,32]]. In this study, we applied QDs-based fluorescent probe to indirectly label glycan epitopes, and then *in situ* observed two representative wall polysaccharides (pectin and xylan) in the transverse sections of rice stem. Hence, a new method has been established to *in situ* visualize polysaccharides and lignin distributions in various types of cells in stem tissue under different chemical pretreatments, providing a powerful tool to explore wall polymer functions during plant growth *in vivo* and biomass process *in vitro*.

2. Materials and methods

2.1. Sample collection and QDs preparation

Rice cultivar (Nipponbare, NPB) was collected from a previously described field trial [16]. Rice sections (3 mm–5 mm) were cut from the upper second internode: (1) 5 μm thick transverse sections embedded in paraplast plus for immunolabeling and (2) 100 μm thick transverse sections used for phloroglucinol staining and scanning electron microscopic (SEM) observation. The QDs (CdSe/ZnS, 610 nm) and QD-labeled goat anti-mouse IgG were obtained from the company (Beijing Najing Biotechnology co., Ltd). The synthetic process of QDs and QD-labeled goat anti-mouse IgG can refer to the methods described by Wang et al. [33] and East et al. [34] respectively. The hydrodynamic diameters and spectra were characterized before and after conjugating the goat anti-mouse IgG to QDs, and there is little effect on the characteristics of QDs (Figs. S1 and S2. Data provided by the company). In addition, there is no impact on the binding activity between QD-labeled goat anti-mouse IgG and mouse IgG (Fig. S3. Data provided by the company).

2.2. Chemical pretreatment and immunolabeling with QDs for wall polysaccharide detection

Paraffin sections were de-waxed with xylene and rehydrated through an ethanol series from 100% to 0%. Sections were then washed extensively in PBS, incubated with 5-fold dilution of cell wall glycan-directed monoclonal antibodies (mAbs) followed by 200-fold and 100-fold dilution of anti-mouse IgG linked to fluorescein isothiocyanate (FITC) or QDs respectively. Two glycan-directed mAbs were used in this study. CCRC-M38 recognizes epitopes in de-esterified homogalacturonan (pectin), and CCRC-M147 recognizes xylan. Samples were washed at least three times as described [16].

Stem sections were subjected to chemical treatment with 0.5 M NaOH at 25 °C for 2 h, or with 1% H_2SO_4 at 70 °C for 1 h, and then neutralized by at least three washes with distilled water until pH 7.0. After pretreatment, the stem sections were incubated in 3% (w/v) MP/PBS, and diluted secondary antibody solutions for 1.5 h. Samples were then washed with PBS (three times) for at least 5 min each, and incubated either with a 200-fold diluted secondary antibody (Alexa Fluor 488 anti-mouse IgG, Invitrogen, A11001) linked to fluorescein isothiocyanate (FITC) in PBS for 2 h or with a 100-fold diluted secondary antibody linked to QDs in PBS for 4 h in darkness. Conditions of all experiments were described in Table 1. All samples were carried out in triplicate.

2.3. Histochemical staining of lignin

Stem sections were stained with phloroglucinol solution (1%, v/v) for 5 min, soaked in concentrated HCl, and immediately photographed under bright field. The pretreated samples were collected as described above. All samples were carried out in triplicate.

2.4. Fluorescence imaging

FITC fluorescence was observed with an Olympus BX61 microscope equipped with epifluorescence optics. Images were captured with a Hamamatsu ORCA285 camera using Improvision Velocity software. QDs fluorescence was visualized by an Olympus IX71 inverted microscope equipped with DP72 camera using cellSens software. Fluorescence filter cubes including U-MWB2 (excitation: 460 nm–490 nm; emission: 520 nm) and U-MWU2 (excitation: 330 nm–385 nm; emission: 425 nm). At least three micrographs for each sample were captured at the same exposure time.

2.5. Colorimetric assay of hexoses, pentoses and uronic acids

The samples were incubated with distilled water at 25 °C for 1 h to remove soluble sugars prior to acid and alkali pretreatment. The UV–VIS spectrometer (MAPADA V-1100D) was used for the absorbance reading. Hexoses were detected using the anthrone/H_2SO_4 method, and pentoses were measured using the orcinol/HCl method [35]. The standard curves for hexoses and pentoses were drawn using D-glucose and D-xylose as standards (purchased from Sinopharm Chemical Reagent Co., Ltd.) respectively. Because high pentose levels can affect the absorbance reading at 620 nm for hexose assay, deduction from the pentose reading at 660 nm was carried out for final hexose calculation. A series of xylose concentrations were analyzed for plotting the standard curve referred to for the deduction, which was verified by gas chromatography–mass spectrometry (GC–MS) analysis. Total uronic acids were assayed using *m*-hydroxybiphenyl/NaOH method [36]. All samples were carried out in triplicate.

2.6. Scanning electron microscopic (SEM) observation

The sections were pretreated with 0.5 M NaOH or 1% H_2SO_4 as described above and washed with distilled water until pH 7.0. Then they were soaked in glutaraldehyde for 3 h and dehydrated through an ethanol series from 0% to 100%. After drying at room temperature, the samples were sputter-coated with gold. SEM (Hitachi JSM-6390/LV) was conducted using the protocols described by Wang and coworkers [36].

Table 1
Information of FITC and QDs immunolabeling of transverse sections of rice stem with two glycan-directed antibodies after different chemical pretreatments.

Pretreatment	Primary antibody	Secondary antibody	Time (h)	Secondary antibody dilution
–	CCRC-M38/M147	–	2	–
–	CCRC-M38/M147	FITC	2	1 : 200
0.5 M NaOH 25 °C 2 h	CCRC-M38/M147	FITC	2	1 : 200
1% H2SO4 70 °C 1 h	CCRC-M38/M147	FITC	2	1 : 200
–	CCRC-M38/M147	QDs	4	1 : 100
0.5 M NaOH 25 °C 2 h	CCRC-M38/M147	QDs	4	1 : 100
1% H2SO4 70 °C 1 h	CCRC-M38/M147	QDs	4	1 : 100

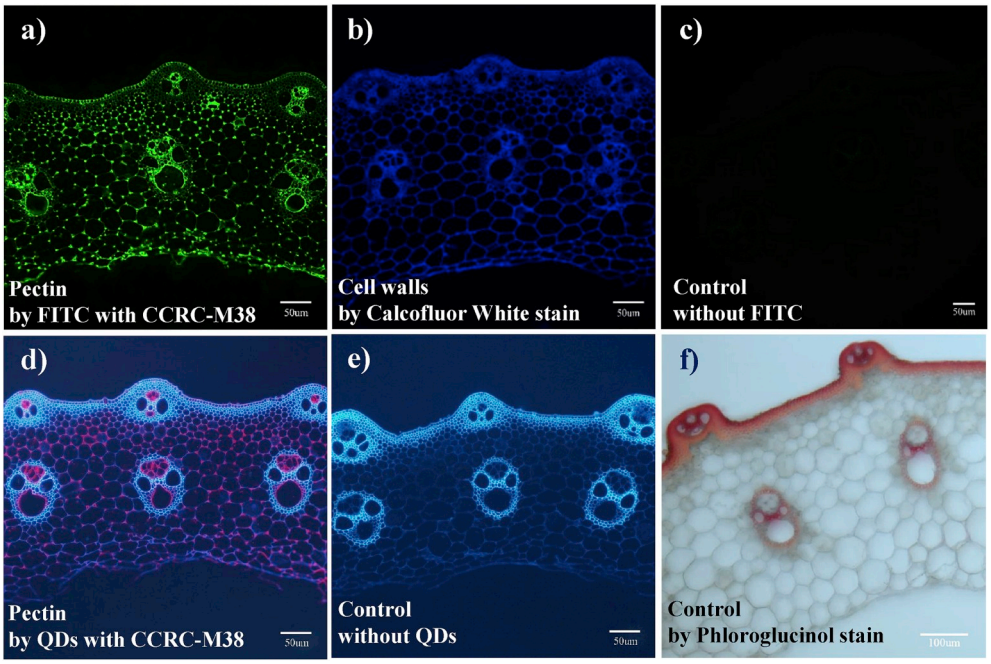

Fig. 1. *In situ* observation of pectin epitopes and lignin deposition in transverse sections of rice stem. (a) Immunofluorescence detection of the binding of CCRC-M38 labeled with FITC (green). (b) Calcofluor White image showing all cell walls. (c) Rice stem sections incubated with buffer in place of secondary antibody as controls. (d) Immunofluorescence detection of the binding of CCRC-M38 labeled with QDs (red) and autofluorescence (blue). (e) Section incubated with buffer in place of secondary antibody as control. (f) Phloroglucinol staining corresponding for lignin deposition. (For interpretation of the references to color in this figure legend, the reader is referred to the Web version of this article.)

3. Results and discussion

3.1. Immunofluorescence detection of pectin epitopes in rice stem

Using glycan-directed immunolabeling approach, this study exhibited pectin (de-esterified homogalacturonan) distribution in the cell walls of transverse sections of rice stem (Fig. 1a), compared to the control showing all cell walls (Fig. 1b) and empty background without fluorescent probes FITC (Fig. 1c). In particular, the immunofluorescence of pectin has a broad distribution in the cell corners of ground tissues, consistent with the previous reports [16].

Despite QDs have been widely used in mammalian and human studies ([28–30]), this labeling technique is little performed to investigate plant wall polysaccharides distribution *in situ*, especially to visualize how biomass processing steps extract wall polymers. In this work, we used the QDs (CdSe/ZnS) to link with the secondary antibodies against the pectin-directed antibody CCRC-M38 and xylan-directed antibody CCRC-M147, and then sorted out the optimal condition for immunolabeling wall polysaccharides *in situ* (Table 1). As comparison with FITC labeling (Fig. 1a), Calcofluor White stain (Fig. 1b), and the control without any probe (Fig. 1c, e), QDs labeling (red fluorescence) showed the strong recognition of pectin around the protoxylem vessels and phloem cells in vascular region, and notably more abundant at cell corners in the parenchyma (Fig. 1d), which was similar to the binding pattern of FITC labeling (Fig. 1a). Hence, the data revealed that the QDs labeling was applicable to visualize pectin epitopes *in situ* in plant cell walls.

Furthermore, histochemical staining of lignin with phloroglucinol-HCl solution was employed to observe lignin distribution patterns of rice cell walls (Fig. 1f), which was extensive in thickened cell walls of the vascular tissue [37]. Meanwhile, the blue autofluorescence (Fig. 1d and e) exhibits similar patterns of lignin distribution across the stem with red stain by phloroglucinol-HCl method, indicating that this QDs labeling technique could not only be sensitive for *in situ* visualization of pectic polysaccharides, but it was also available to highlight lignin distribution at the cellular level in the same dissection of rice stem.

3.2. Characteristics of xylan distribution in rice stem

Because the QDs labeling technique was able to simultaneously characterize pectin and lignin in different types of cells in one stem dissection, this study further *in situ* observed xylan distribution, a major type of hemicellulose in rice cell walls. Using xylan-directed mAb CCRC-M147, the results showed that CCRC-M147 was bound to the cell walls in the vascular bundles (Fig. 2a), consistent with the previous findings [16]. However, unlike the broad distribution of CCRC-M38 HG epitope in rice stem tissues, the binding pattern of CCRC-M147 xylan was found to be different. Notably, the distribution pattern of xylan recognized by CCRC-M147 with QDs in red fluorescence was similarly observed in the vascular bundles, but the QDs dissection also presented all other cell morphogenesis by autofluorescence in blue (Fig. 2b). Therefore, the results confirmed that the established QDs approach

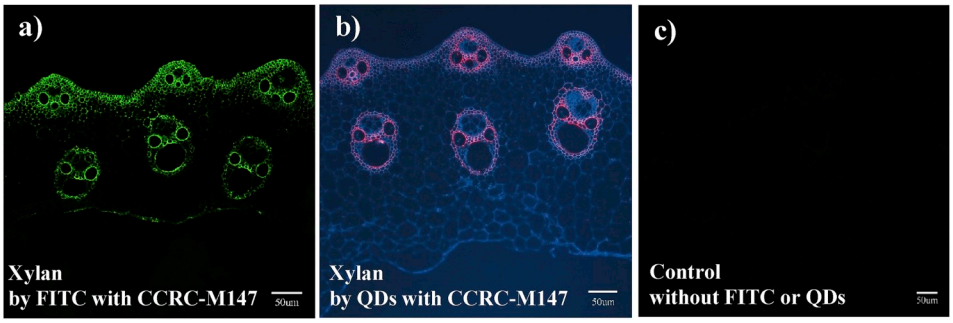

Fig. 2. Immunofluorescence detection of xylan epitopes in transverse sections of rice stem. (a) The binding of CCRC-M38 labeled with FITC (green). (b) The binding of CCRC-M38 labeled with QDs (red) and autofluorescence (blue). (c) Section incubated with buffer in place of secondary antibody using U-MWB2 fluorescence filter as control. (For interpretation of the references to color in this figure legend, the reader is referred to the Web version of this article.)

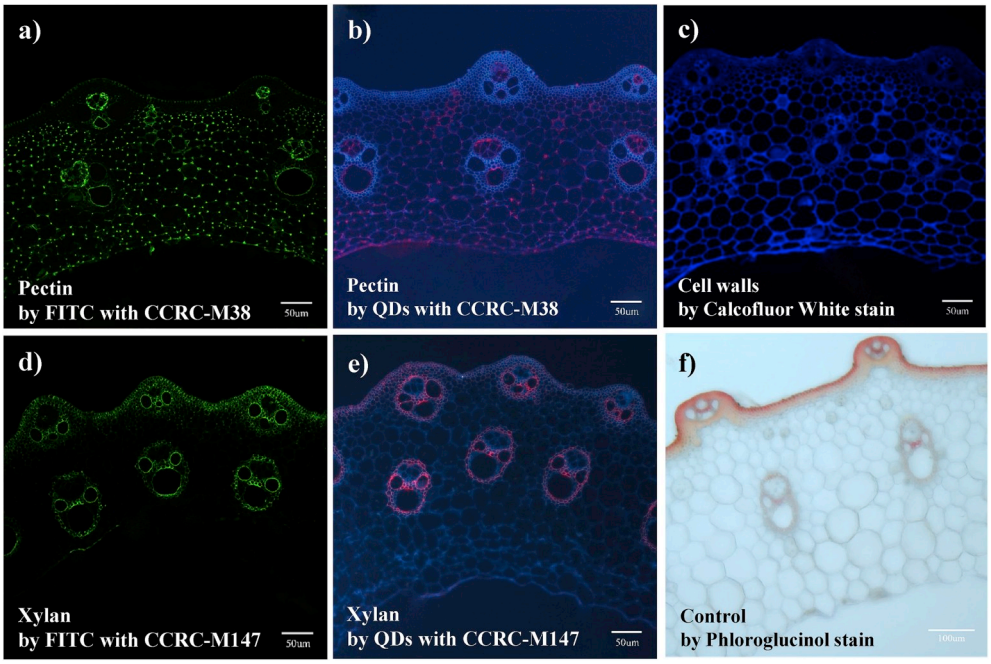

Fig. 3. *In situ* observation of different wall polymers in transverse sections of rice stem after 0.5 M NaOH pretreatment. (a) Immunofluorescence detection of the binding of CCRC-M38 labeled with FITC (green). (b) Immunofluorescence detection of the binding of CCRC-M38 labeled with QDs (red) and auto-fluorescence (blue). (c) Calcofluor White image showing all cell walls. (d) Immunofluorescence detection of the binding of CCRC-M147 labeled with FITC (green). (e) Immunofluorescence detection of the binding of CCRC-M147 labeled with QDs (red) and autofluorescence (blue). (f) Phloroglucinol staining corresponding for lignin deposition. (For interpretation of the references to color in this figure legend, the reader is referred to the Web version of this article.)

should be applicable to characterize all major wall polysaccharides and lignin, together with viewing of cell morphogenesis.

It also suggested that the QDs should be more applicable to directly label the glycan-directed mAbs bound to pectic polysaccharides. Since the QDs have unique spectral properties, QDs with distinct sizes have different colors [21]. The established QDs labeling technique could be applied to monitor multiple wall polysaccharides at the cellular level in real time [24,25]. By contrast, the FITC labeling was only allowed to observe single polysaccharide at one dissection, indicating that the QDs labeling should be more conventional for simultaneously visualizing multiple wall polysaccharides *in situ*.

3.3. Distinct destruction of wall polysaccharides and lignin from alkali pretreatment

As an initial step for biomass saccharification and bioethanol production, alkali pretreatment of biomass has been broadly used to partially extract wall polymers by disassociating hydrogen bonds among polymers and cellulose microfibrils [7,38]. In the present work, we used both FITC labeling and QDs labeling techniques to visualize wall polymer destruction after mild pretreatment (0.5 M NaOH at 25 °C for 2 h) of rice stem dissection (Fig. 3). Compared to the control without any pretreatment (Fig. 1a, d), the alkali pretreated stem dissections showed either relatively weaker fluorescence for both FITC (green) and QDs (red) labeled pectin epitopes (Fig. 3a and b), indicating that pectic polysaccharides should be partially extracted from mild alkali pretreatment as previously reported [13,16]. Meanwhile, chemical analysis indicated that a much higher proportion of uronic acids was extracted than those of hexoses and pentoses from the mild alkali pretreatment (Fig. 5a). As uronic acids are typical components of pectic polysaccharides [36,39], the data confirmed a major extraction of pectin from the alkali pretreatment. In addition, we observed relatively weaker autofluorescence and reduced lignin distribution using phloroglucinol stain (Fig. 3b, f), compared to the controls (Fig. 1d, f), which was consistent with the previous reports about effective lignin extraction with alkali pretreatments [38]. Hence, this study further demonstrated that the established QDs technique could be applicable to *in situ* observe distinct destruction of pectic polysaccharides and lignin in different types of plant cell walls at one alkali-pretreated stem dissection.

Furthermore, this study observed slightly reduced intensity of fluorescence signal by FITC labeling or QDs labeling bound to xylan epitopes from the mild alkali pretreatment (Fig. 3d and e), compared to the controls (Fig. 2a and b). Previous studies have shown that CCRC-M147 could detect different degree of polymerization homoxylan and substituted xylan regions [15,40]. As small amounts of pentoses were examined from the alkali pretreatment (Fig. 5a), the application of alkali pretreatment is likely to remove partial xylan epitopes, resulting in observation of weaker fluorescence signal by FITC or QDs probe. Taken together, this study revealed that the QDs technology is of broad application for observation of distinct destruction of wall polysaccharides and lignin at the same alkali-pretreated stem tissues.

3.4. Enhanced insights into wall polysaccharide distribution after acid pretreatment with stem tissues

Acid pretreatment has been applied to partially digest non-cellulosic polysaccharides at high temperature [38]. However, this study performed relatively mild acid pretreatment (1% H_2SO_4 at 70 °C for 1 h), in order to maintain cell integrity of stem dissection (Fig. 4). Unexpectedly, the acid pretreated stem dissections even showed stronger fluorescence of FITC labeling and QDs labeling respectively recognized either pectin epitopes (Fig. 4a and b) and xylan epitopes (Fig. 4d and e), compared to their controls (Figs. 1 and 2), which was contrast with the findings of the alkali pretreatment as described above. However, despite this study conducted relatively mild acid pretreatment, it led to much more pentoses and hexoses extractions than those of the alkali pretreatment (Fig. 5a and b), suggesting that the acid pretreatment remained efficient for non-cellulosic polysaccharides extraction. Therefore, in terms of the enhanced fluorescence signal for both FITC labeling and QDs labeling observed in the acid pretreated stem tissues, we presumed that the acid pretreatment performed in this study may be favor for extraction of other minor non-cellulosic polysaccharides that are not tightly associated with wall networks, resulting in exposure of more epitopes of pectin and xylan for binding the mAbs with FITC labeling or QDs labeling [41]. In addition, because it has been characterized that lignin is resistant to the acid pretreatments [38], we did not observe much altered autofluorescence and phloroglucinol stain corresponding for lignin distribution (Fig. 4b, f). Hence, this study indicated that the QDs labeling technique could observe dynamical

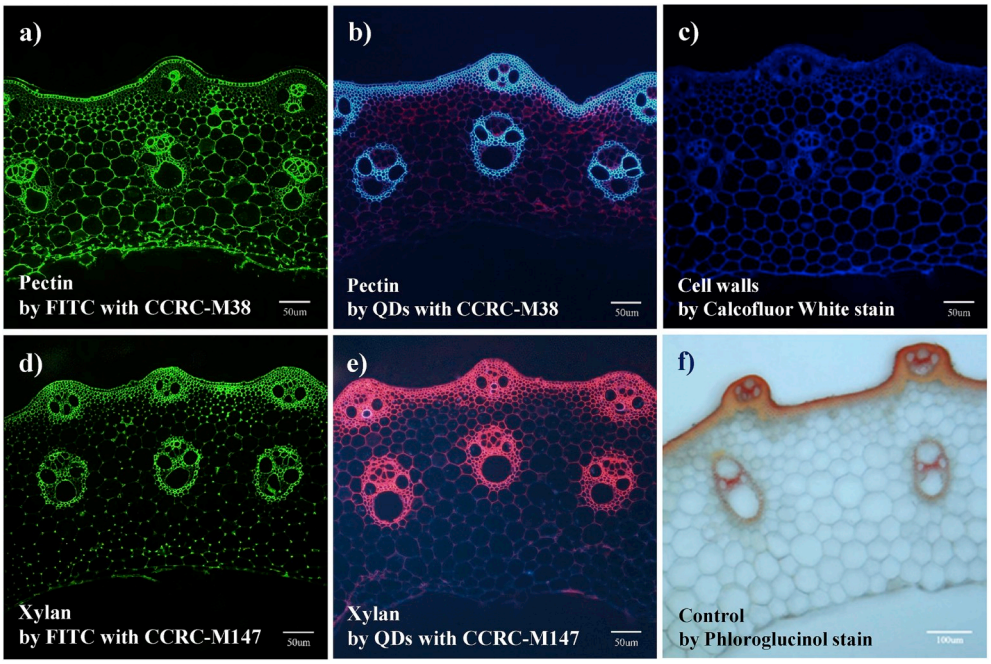

Fig. 4. *In situ* observation of different wall polymers in transverse sections of rice stem after 1% H2SO4 pretreatment. (a) Immunofluorescence detection of the binding of CCRC-M38 labeled with FITC (green). (b) Immunofluorescence detection of the binding of CCRC-M38 labeled with QDs (red) and autofluorescence (blue). (c) Calcofluor White image showing all cell walls. (d) Immunofluorescence detection of the binding of CCRC-M147 labeled with FITC (green). (e) Immunofluorescence detection of the binding of CCRC-M147 labeled with QDs (red) and auto-fluorescence (blue). (f) Phloroglucinol staining corresponding for lignin deposition. (For interpretation of the references to color in this figure legend, the reader is referred to the Web version of this article.)

destruction of wall polymers *in situ* during the acid pretreatment of stem tissues.

3.5. Significantly altered cell wall topology under acid pretreatment

To understand why the alkali and acid pretreatments led to a distinctive profiling of pectin and xylan under both FITC labeling and QDs labeling, this study observed cell wall surfaces in rice stem dissections using SEM (Fig. 6). Compared to the control (without pretreatment) (Fig. 6a), the mild alkali pretreated dissection showed a similar cell wall surface (Fig. 6b), whereas the acid pretreated dissection exhibited a very rough face (Fig. 6c), consistent with much more sugars released from the acid pretreatment. With respect to the coarse face of the acid pretreated stem dissection, we presumed that it should cause an efficient penetration of FITC and QDs into cell walls, interpreting why this study observed stronger fluorescence signal of FITC labeling and QDs labeling corresponding for pectin and xylan. Because alkali pretreatment mainly acts as peeling of wall polymers [42], it may interpret why the mild alkali pretreated dissection did not show a rough surface in this study. However, as described above, the QDs labeling technique could be more sensitive to profile wall polymers distribution and destruction in the stem dissections, compared to the SEM observation of the chemical pretreated stem tissues.

4. Conclusion

Using FITC labeling as a control, this study well established QDs labeling approach to *in situ* observe two major wall polysaccharides distribution in different types of cells in rice stem, coupled with lignin view at the same dissection. The established QDs labeling was further demonstrated to be specifically sensitive for profiling wall polymers destruction distinctive from alkali and acid pretreatments with stem dissections. Future work will be required for using QDs probes to directly label glycan-directed mAbs to visualize multiple plant cell wall polysaccharides simultaneously. Hence, this study has found out a powerful tool either to explore wall polymer roles in biomass processing for biofuel production or to investigate plant cell wall structure and function in plant growth and development.

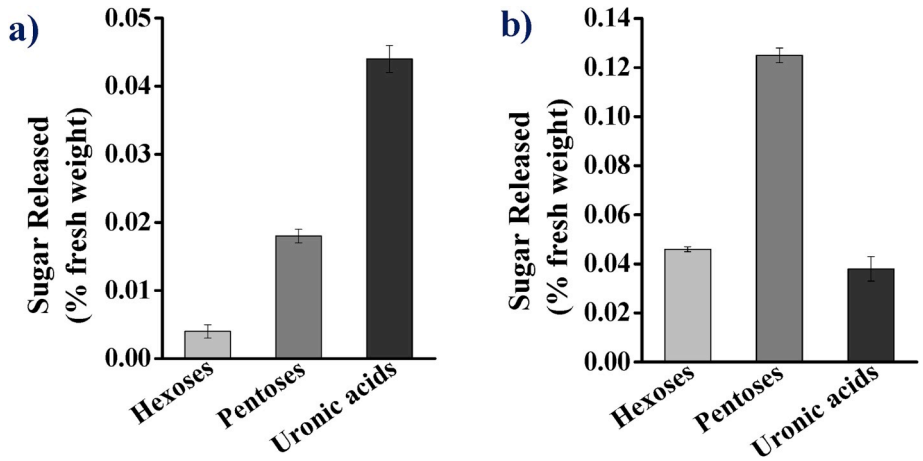

Fig. 5. Hexoses, pentoses and uronic acids yields released from alkali and acid pretreatment in transverse sections of rice stems. (a) After 0.5 M NaOH pretreatment. (b) After 1% H2SO4 pretreatment.

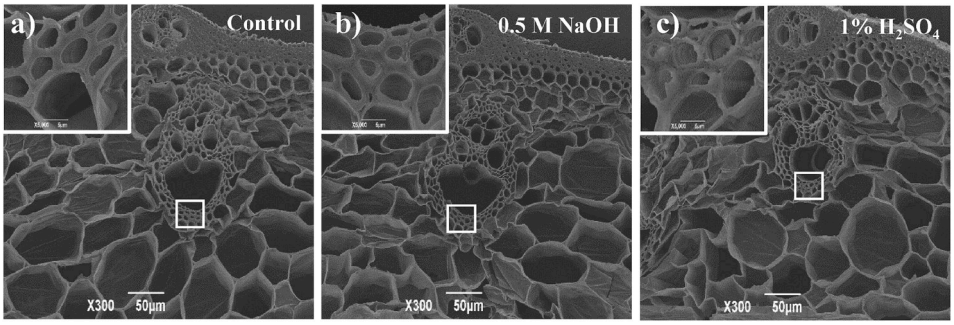

Fig. 6. SEM images of rice cell wall surface after alkali and acid pretreatment. (a) Without pretreatment. (b) After 0.5 M NaOH pretreatment. (c) After 1% H2SO4 pretreatment. The area in the white square highlights the morphology alteration between different chemical pretreatments.

Acknowledgements

This work was supported in part by grants from the National Science Foundation of China (31670296, 31571721), the Project of Hubei University of Arts and Science (XKQ2018006), and Open Grant of the Key Laboratory of Development and Application of Rural Renewable Energy, Ministry of Agriculture and Rural Affairs to Y. Wang. Generation of the CCRC-M38 monoclonal antibody used in this work was supported by a grant from the NSF Plant Genome Program (DBI-0421683), and QD (CdTe/ZnS, 610 nm) linked with secondary antibody was generated by Beijing Najing Biotechnology Co., Ltd.

Appendix A. Supplementary data

Supplementary data to this article can be found online at https://doi.org/10.1016/j.talanta.2019.120452.

References

[1] A.J. Ragauskas, C.K. Williams, B.H. Davison, G. Britovsek, J. Cairney, C.A. Eckert, W.J. Frederick Jr., J.P. Hallett, D.J. Leak, C.L. Liotta, J.R. Mielenz, R. Murphy, R. Templer, T. Tschaplinski, The path forward for biofuels and biomaterials, Science 311 (2006) 484–489, https://doi.org/10.1126/science.1114736.

[2] E.R. Lampugnani, G.A. Khan, M. Somssich, S. Persson, Building a plant cell wall at a glance, J. Cell Sci. 131 (2018) jcs207373, https://doi.org/10.1242/jcs.207373.

[3] Y. Wang, C. Fan, H. Hu, Y. Li, D. Sun, Y. Wang, L. Peng, Genetic modification of plant cell walls to enhance biomass yield and biofuel production in bioenergy crops, Biotechnol. Adv. 34 (2016) 997–1017, https://doi.org/10.1016/j.biotechadv.2016.06.001.

[4] F. Li, G. Xie, J. Huang, R. Zhang, Y. Li, M. Zhang, Y. Wang, A. Li, X. Li, T. Xia, C. Qu, F. Hu, A.J. Ragauskas, L. Peng, OsCESA9 conserved-site mutation leads to largely enhanced plant lodging resistance and biomass enzymatic saccharification by reducing cellulose DP and crystallinity in rice, Plant Biotechnol. J. 15 (2017) 1093–1104, https://doi.org/10.1111/pbi.12700.

[5] Y. Li, P. Liu, J. Huang, R. Zhang, Z. Hu, S. Feng, Y. Wang, L. Wang, T. Xia, L. Peng, Mild chemical pretreatments are sufficient for bioethanol production in transgenic rice straws overproducing glucosidase, Green Chem. 20 (2018) 2047–2056, https://doi.org/10.1039/C8GC00694F.

[6] Z. Hu, G. Zhang, A. Muhammad, R.A. Samad, Y. Wang, J.D. Walton, Y. He, L. Peng, L. Wang, Genetic loci simultaneously controlling lignin monomers and biomass digestibility of rice straw, Sci. Rep. 8 (2018) 3636, https://doi.org/10.1038/s41598-018-21741-y.

[7] M. Li, S. Si, B. Hao, Y. Zha, C. Wan, S. Hong, Y. Kang, J. Jia, J. Zhang, M. Li, C. Zhao, Y. Tu, S. Zhou, L. Peng, Mild alkali-pretreatment effectively extracts guaiacyl-rich lignin for high lignocellulose digestibility coupled with largely diminishing yeast fermentation inhibitors in *Miscanthus*, Bioresour. Technol. 169 (2014) 447–454, https://doi.org/10.1016/j.biortech.2014.07.017.

[8] Zahoor, Y. Tu, L. Wang, T. Xia, D. Sun, S. Zhou, Y. Wang, Y. Li, H. Zhang, T. Zhang, M. Madadi, L. Peng, Mild chemical pretreatments are sufficient for complete saccharification of steam-exploded residues and high ethanol production in desirable wheat accessions, Bioresour. Technol. 243 (2017) 319–326, https://doi.org/10.1016/j.biortech.2017.06.111.

[9] J.D. Demartini, S. Pattathil, U. Avci, K. Szekalski, K. Mazumder, M.G. Hahn, C.E. Wyman, Application of monoclonal antibodies to investigate plant cell wall deconstruction for biofuels production, Energy Environ. Sci. 4 (2011) 4332–4339, https://doi.org/10.1039/C1EE02112E.

[10] A. Endler, C. Kesten, R. Schneider, Y. Zhang, A. Ivakov, A. Froehlich, N. Funke, S. Persson, A mechanism for sustained cellulose synthesis during salt stress, Cell 162 (2015) 1353–1364, https://doi.org/10.1016/j.cell.2015.08.028.

[11] M.G. Rydahl, A.R. Hansen, S.K. Kraćun, J. Mravec, Report on the current inventory of the toolbox for plant cell wall analysis: proteinaceous and small molecular probes, Front. Plant Sci. 9 (2018) 581, https://doi.org/10.3389/fpls.2018.00581.

[12] S. Persson, K.H. Caffall, G. Freshour, M.T. Hilley, S. Bauer, P. Poindexter, M.G. Hahn, D. Mohnen, C. Somerville, The *Arabidopsis* irregular xylem8 mutant is deficient in glucuronoxylan and homogalacturonan, which are essential for secondary cell wall integrity, Plant Cell 19 (2007) 237–255, https://doi.org/10.1105/tpc.106.047720.

[13] S. Pattathil, U. Avci, D. Baldwin, A.G. Swennes, J.A. McGill, Z. Popper, T. Bootten, A. Albert, R.H. Davis, C. Chennareddy, R. Dong, B. O'Shea, R. Rossi, C. Leoff, G. Freshour, R. Narra, M. O'Neil, W.S. York, M.G. Hahn, A comprehensive toolkit of plant cell wall glycan-directed monoclonal antibodies, Plant Physiol. 153 (2010) 514–525, https://doi.org/10.1104/pp.109.151985.

[14] U. Avci, S. Pattathil, M.G. Hahn, Immunological approaches to plant cell wall and biomass characterization: immunolocalization of glycan epitopes, Methods Mol. Biol. 908 (2012) 73–82, https://doi.org/10.1007/978-1-61779-956-3_7.

[15] A.G. Peralta, S. Venkatachalam, S.C. Stone, S. Pattathil, Xylan epitope profiling: an enhanced approach to study organ development-dependent changes in xylan structure, biosynthesis, and distribution in plant cell walls, Biotechnol. Biofuels 10 (2017) 245, https://doi.org/10.1186/s13068-017-0935-5.

[16] Y. Li, J. Zhuo, P. Liu, P. Chen, H. Hu, Y. Wang, S. Zhou, Y. Tu, L. Peng, Y. Wang, Distinct wall polymer deconstruction for high biomass digestibility under chemical pretreatment in *Miscanthus*, and rice, Carbohydr. Polym. 192 (2018) 273–281, https://doi.org/10.1016/j.carbpol.2018.03.013.

[17] B. Dubertret, P. Skourides, D.J. Norris, V. Noireaux, A.H. Brivanlou, A. Libchaber, In vivo imaging of quantum dots encapsulated in phospholipid micelles, Science 298 (2002) 1759–1762, https://doi.org/10.1126/science.1077194.

[18] J.A. Kloepfer, R.E. Mielke, M.S. Wong, K.H. Nealson, G. Stucky, J.L. Nadeau, Quantum dots as strain- and metabolism-specific microbiological labels, Appl. Environ. Microbiol. 69 (2003) 4205–4213, https://doi.org/10.1128/aem.69.7.4205-4213.2003.

[19] J.K. Jaiswal, E.R. Goldman, H. Mattoussi, S.M. Simon, Use of quantum dots for live cell imaging, Nat. Methods 1 (2004) 73–78, https://doi.org/10.1038/nmeth1004-73.

[20] I.L. Medintz, H.T. Uyeda, E.R. Goldman, H. Mattoussi, Quantum dot bioconjugates for imaging, labelling and sensing, Nat. Mater. 4 (2005) 435–446, https://doi.org/10.1038/nmat1390.

[21] G. Paës, Fluorescent probes for exploring plant cell wall deconstruction: a review, Molecules 19 (2014) 9380–9402, https://doi.org/10.3390/molecules19079380.

[22] Y. He, H. Xu, C. Chen, J. Peng, H. Tang, Z. Zhang, Y. Li, D. Pang, In situ spectral imaging of marker proteins in gastric cancer with near-infrared and visible quantum dots probes, Talanta 85 (2011) 136–141, https://doi.org/10.1016/j.talanta.2011.03.035.

[23] L. Chen, A. Willoughby, J. Zhang, Luminescent gelatin nanospheres by encapsulating CdSe quantum dots, Luminescence 29 (2014) 74–78, https://doi.org/10.1002/bio.2505.

[24] Q. Xu, M.P. Tucker, P. Arenkiel, X. Ai, G. Rumbles, J. Sugiyama, M.E. Himmel, S.Y. Ding, Labeling the planar face of crystalline cellulose using quantum dots directed by type-I carbohydrate-binding modules, Cellulose 16 (2009) 19–26, https://doi.org/10.1007/s10570-008-9234-4.

[25] J.M. Feugang, R.C. Youngblood, J.M. Greene, S.T. Willard, P.L. Ryan, Self-illuminating quantum dots for non-invasive bioluminescence imaging of mammalian gametes, J. Nanobiotechnol. 13 (2015) 38, https://doi.org/10.1186/s12951-015-0097-1.

[26] W.C. Chan, S. Nie, Quantum dot bioconjugates for ultrasensitive nonisotopic detection, Science 281 (1998) 2016–2018, https://doi.org/10.1126/science.281.5385.2016.

[27] M. Bruchez, M. Moronne, P. Gin, S. Weiss, A.P. Alivisatos, Semiconductor nanocrystals as fluorescent biological labels, Science 281 (1998) 2013–2016, https://doi.org/10.1126/science.281.5385.2013.

[28] X. Ai, L. Niu, Y. Li, F. Yang, X. Su, A novel β-cyclodextrin-QDs optical biosensor for the determination of amantadine and its application in cell imaging, Talanta 99 (2012) 409–414, https://doi.org/10.1016/j.talanta.2012.05.072.

[29] L.Y. Guan, Y.Q. Li, S. Lin, M.Z. Zhang, J. Chen, Z.Y. Ma, Y.D. Zhao, Characterization of CdTe/CdSe quantum dots-transferrin fluorescent probes for cellular labeling, Anal. Chim. Acta 741 (2012) 86–92, https://doi.org/10.1016/j.aca.2012.06.043.

[30] F. Yang, Z. Xu, J. Wang, F. Zan, C. Dong, J. Ren, Microwave-assisted aqueous

synthesis of new quaternary-alloyed CdSe/TeS quantum dots; and their bioapplications in targeted imaging of cancer cells, Luminescence 28 (2013) 392–400, https://doi.org/10.1002/bio.2395.
[31] Y. Hu, J. Li, L. Ma, Q. Peng, W. Feng, L. Zhang, S. He, F. Yang, J. Huang, L. Li, High efficiency transport of quantum dots into plant roots with the aid of Silwet L-77, Plant Physiol. Biochem. 48 (2010) 703–709, https://doi.org/10.1016/j.plaphy.2010.04.001.
[32] D. Djikanović, A. Kalauzi, M. Jeremić, J. Xu, M. Mićić, J.D. Whyte, R.M. Leblanc, K. Radotić, Interaction of the CdSe quantum dots with plant cell walls, Colloids Surf., B 91 (2012) 41–47, https://doi.org/10.1016/j.colsurfb.2011.10.032.
[33] Y. Wang, M. Yu, K. Yang, J. Lu, L. Chen, Simple synthesis of luminescent CdSe quantum dots from ascorbic acid and selenium dioxide, Luminescence 30 (2016) 1375–1379, https://doi.org/10.1002/bio.2909.
[34] D.A. East, M. Todd, I.J. Bruce, Quantum dot–antibody conjugates via carbodiimide-mediated coupling for cellular imaging, Methods Mol. Biol. 1199 (2014) 67–83, https://doi.org/10.1007/978-1-4939-1280-3_5.
[35] J. Huang, T. Xia, A. Li, B. Yu, Q. Li, Y. Tu, W. Zhang, Z. Yi, L. Peng, A rapid and consistent near infrared spectroscopic assay for biomass enzymatic digestibility upon various physical and chemical pretreatments in *Miscanthus*, Bioresour. Technol. 121 (2012) 274–281, https://doi.org/10.1016/j.biortech.2012.06.015.
[36] Y. Wang, J. Huang, Y. Li, K. Xiong, Y. Wang, F. Li, M. Liu, Z. Wu, Y. Tu, L. Peng, Ammonium oxalate-extractable uronic acids positively affect biomass enzymatic digestibility by reducing lignocellulose crystallinity in *Miscanthus*, Bioresour. Technol. 196 (2015) 391–398, https://doi.org/10.1016/j.biortech.2015.07.099.
[37] R. Zhong, A. Ripperger, Z.H. Ye, Ectopic distribution of lignin in the pith of stems of two *Arabidopsis* mutants, Plant Physiol. 123 (2000) 59–69, https://doi.org/10.1104/pp.123.1.59.
[38] S. Si, Y. Chen, C. Fan, H. Hu, Y. Li, J. Huang, H. Liao, B. Hao, Q. Li, L. Peng, Y. Tu, Lignin extraction distinctively enhances biomass enzymatic saccharification in hemicelluloses-rich *Miscanthus* species under various alkali and acid pretreatments, Bioresour. Technol. 183 (2015) 248–254, https://doi.org/10.1016/j.biortech.2015.02.031.
[39] D. Mohnen, Pectin structure and biosynthesis, Curr. Opin. Plant Biol. 11 (2008) 266–277, https://doi.org/10.1016/j.pbi.2008.03.006.
[40] S. Pattathil, U. Avci, J.S. Miller, M.G. Hahn, Immunological approaches to plant cell wall and biomass characterization: glycome profiling, Methods Mol. Biol. 908 (2012) 61–72, https://doi.org/10.1007/978-1-61779-956-3_6.
[41] S.E. Marcus, Y. Verhertbruggen, C. Hervé, J.J. Ordaz-Ortiz, V. Farkas, H.L. Pedersen, W.G. Willats, J.P. Knox, Pectic homogalacturonan masks abundant sets of xyloglucan epitopes in plant cell walls, BMC Plant Biol. 8 (2008) 60, https://doi.org/10.1186/1471-2229-8-60.
[42] A.T.W.M. Hendriks, G. Zeeman, Pretreatments to enhance digestibility of lignocellulosic biomass, Bioresour. Technol. 100 (2008) 10–18, https://doi.org/10.1016/j.biortech.2008.05.027.